Neural Circuit Mechanism of Decision Uncertainty and Change-of-Mind

Nadim A A Atiya[1], Iñaki Rañó[1], Girijesh Prasad[1], and KongFatt Wong-Lin[1,*]

[1]Intelligent Systems Research Centre, School of Computing, Engineering and Intelligent Systems, Ulster University, Magee campus, Derry~Londonderry, Northern Ireland, UK

*Corresponding author: k.wong-lin@ulster.ac.uk (KongFatt Wong-Lin)

Acknowledgements

We thank D. O'Hora and A. Zgonnikov for helpful discussions. We also thank P.T. Piiroinen, J. Zhang, S.P. Kelly and R.G. O'Connell for insightful discussion during the early phase of the project, and W.P. Boyce and A. Joshi for critical reading of the manuscript. This work was supported by the Ulster University Vice-Chancellor's Research Scholarship Award (N.A.), Northern Ireland Functional Brain Mapping Project 1303/101154803 funded by InvestNI and the Ulster University (G.P. and K.W.-L.), and The Royal Society International Exchange Scheme under grant IE151293 (I.R. and K.W.-L.). K.W.-L. was further supported by BBSRC (BB/P003427/1), COST Action Open Multiscale Systems Medicine (OpenMultiMed) supported by COST (European Cooperation in Science and Technology), and The Royal Society - NSFC International Exchanges under grant IE141307.

Author contributions

N.A. and K.W-L. formulated the idea. N.A. and K.W.-L. designed the experiments. N.A. performed and analyzed most of the experiments. N.A. and K.W.-L. analyzed the data. I.R. and G.P. provided additional suggestions relevant to the experiments and analysis. N.A. and K.W.-L. wrote the original draft of the paper. All authors reviewed and edited the paper.

Competing interests

The authors declare no competing financial interests.

Abstract

Decision-making is often accompanied by a degree of confidence on whether a choice is correct. Decision uncertainty, or lack in confidence, may lead to change-of-mind. Studies have identified the behavioural characteristics associated with decision confidence or change-of-mind, and their neural correlates. Although several theoretical accounts have been proposed, there is no neural model that can compute decision uncertainty and explain its effects on change-of-mind. We propose a neuronal circuit model that computes decision uncertainty while accounting for a variety of behavioural and neural data of decision confidence and change-of-mind, including testable model predictions. Our theoretical analysis suggests that change-of-mind occurs due to the presence of a transient uncertainty-induced choice-neutral stable steady state and noisy fluctuation within the neuronal network. Our distributed network model indicates that the neural basis of change-of-mind is more distinctively identified in motor-based neurons. Overall, our model provides a framework that unifies decision confidence and change-of-mind.

The decisions we make are often accompanied with a degree of uncertainty – how likely a decision will be correct[1–3]. Some decisions are more difficult than others, inducing internal conflict that may lead to reconsideration or change-of-mind[4,5]. Likewise, challenging decisions are associated with higher uncertainty, more errors and longer response times[1,6,7]. This high uncertainty could also result in subsequent behavioural adjustments, affecting how quickly and accurately we make consecutive decisions[8,9]. Several theoretical and experimental accounts posit that uncertainty is computed while making decisions[6,7,10–15]. However, how decision uncertainty is encoded in the brain and the neural mechanism by which it affects changes-of-mind and subsequent behavioural adjustments has, so far, remained elusive[16–18].

The neural correlates of decision uncertainty have been gradually revealed in animal and human studies[6,7,13,19–21]. For instance, neural recordings from animals demonstrated strong correlation between lower neuronal activity in the lateral intraparietal (LIP) and high decision uncertainty[7]. Computational models have accounted for this, suggesting that neural responses are represented by probability distributions, where uncertainty can be quantified by evaluating the posterior probability[10,22]. These models, however, imply Bayesian optimality[23], with no consensus on how this optimality emerges from the neurobiology[8,24].

Other experimental studies have shown weaker linkage between choice accuracy and uncertainty-level reporting[6,11,19,25,26]. For instance, patients with lesions in the prefrontal cortex demonstrated poor confidence reporting performance, while choice accuracy was largely unaffected[19]. Several computational models support this view by predicting a dissociation between uncertainty and the formation of perceptual decision[27,28]. For instance, in one model[27], an extension of the drift-diffusion decision-making model (for evidence accumulation) [29,30], the evidence accumulation continues after a decision is reached, and hence a post-decision confidence rating can be provided. Specifically, the parameters controlling the post-decision stage are independent from the ones that control initial decision processing stage.

Changing one's mind has been attributed to processing new evidence that negates a

previous judgement[4]. More recent neurophysiological evidence has shown that some changes-of-mind occur as a result of an internal error-correction mechanism[25], suggesting decision uncertainty plays a role in inducing changes-of-mind[31]. However, the neural mechanism of decision uncertainty (within a single trial or across consecutive ones) and its link to change-of-mind has so far remained ambiguous. In particular, there is no neural circuit model that explains this shared neural mechanism[17].

Within the studies of perceptual decision confidence/uncertainty and change-of-mind, there are some common findings that have been identified. Firstly, more difficult tasks, associated with lower (sensory) evidence quality, lead to higher decision uncertainty, which is also associated with lower choice accuracy[6,10,32]. Secondly, higher decision uncertainty is associated with lower evidence quality of correct choices while counter-intuitively associated with better evidence quality for incorrect choices (forming the often observed "X" pattern) [6,10,32]. Thirdly, changes-of-mind are more likely to occur when the task is more difficult, and more often accompanied by correcting an initial impending error choice – hence more error-to-correct changes than correct-to-error changes[4,33] (although the difference has been shown to vary in some cases[33]). Further, the likelihood of correct changes-of-mind (to the subsequent correct choices) may peak at an intermediate level of task difficulty and then decrease gradually when the task becomes much easier[4,33].

In this work, we developed the first neural circuit computational model that can mechanistically quantify and monitor decision uncertainty, which may subsequently cause a change-of-mind, hence unifying the two areas of study. Our multi-layer recurrent network model not only accounts for the abovementioned key characteristics of decision uncertainty[6,10,32] and change-of-mind[4,33] across a wide variety of experiments, but also sheds light on their neural circuit mechanisms. In particular, using dynamical systems analysis, we show that change-of-mind occurs due to the presence of a transient choice-neutral stable steady state together with noisy fluctuation within the neuronal network. Interestingly, because our model consists of multiple layers of neural integrators, we found that reversal of competing neural activity (neural basis for change-of-mind) is more likely to be more

distinctive for neurons near the motor execution area, without necessarily requiring a clear reversal of neural activity at more upstream sensory or sensorimotor neurons. Further, as our model can directly translate to motor output (positional space), it can explicitly produce early and late change-of-mind behaviours.

Results

Neural circuit model computes decision uncertainty

We propose a novel neural circuit model that can encode, quantify, and monitor decision uncertainty, which we named the decision uncertainty-monitoring module (Fig. 1a, grey box). This specific circuit is built on top of our previous biologically plausible neural circuit model of decision-making that focuses on sensory evidence accumulation[34] (Fig. 1a).

The uncertainty-monitoring module receives input based on the summed sensorimotor neuronal populations activities (Fig. 1a). In particular, the module's neuronal population that encodes low decision uncertainty (Fig. 1a, green circle) integrates these summed activities (Fig. 1a, blue and orange pointed arrows; Methods). This neuronal population in turn inhibits a neighbouring neuronal population that encodes high uncertainty (Fig. 1a, red circle). Hence, decision uncertainty can be continuously monitored. Together, the network structure with these two neuronal populations is reminiscent of a simple cortical column[35].

Further, decision uncertainty information from the uncertainty-monitoring module is continuously fed back to the sensorimotor neuronal populations (Fig. 1a, light blue box), thus providing, effectively, an excitatory feedback mechanism between the two brain systems, which consequently may affect the final decision outcome, and in some instances, even lead to change-of-mind, as we shall demonstrate below. In addition, the neural circuit model also has motor-based neuronal populations either located within the same brain region or downstream in the decision-processing pathway (Fig. 1a, green box). Inputs to these populations are temporally integrated based on the neural firing rate outputs of the associated sensorimotor neuronal populations (Fig. 1a; Methods).

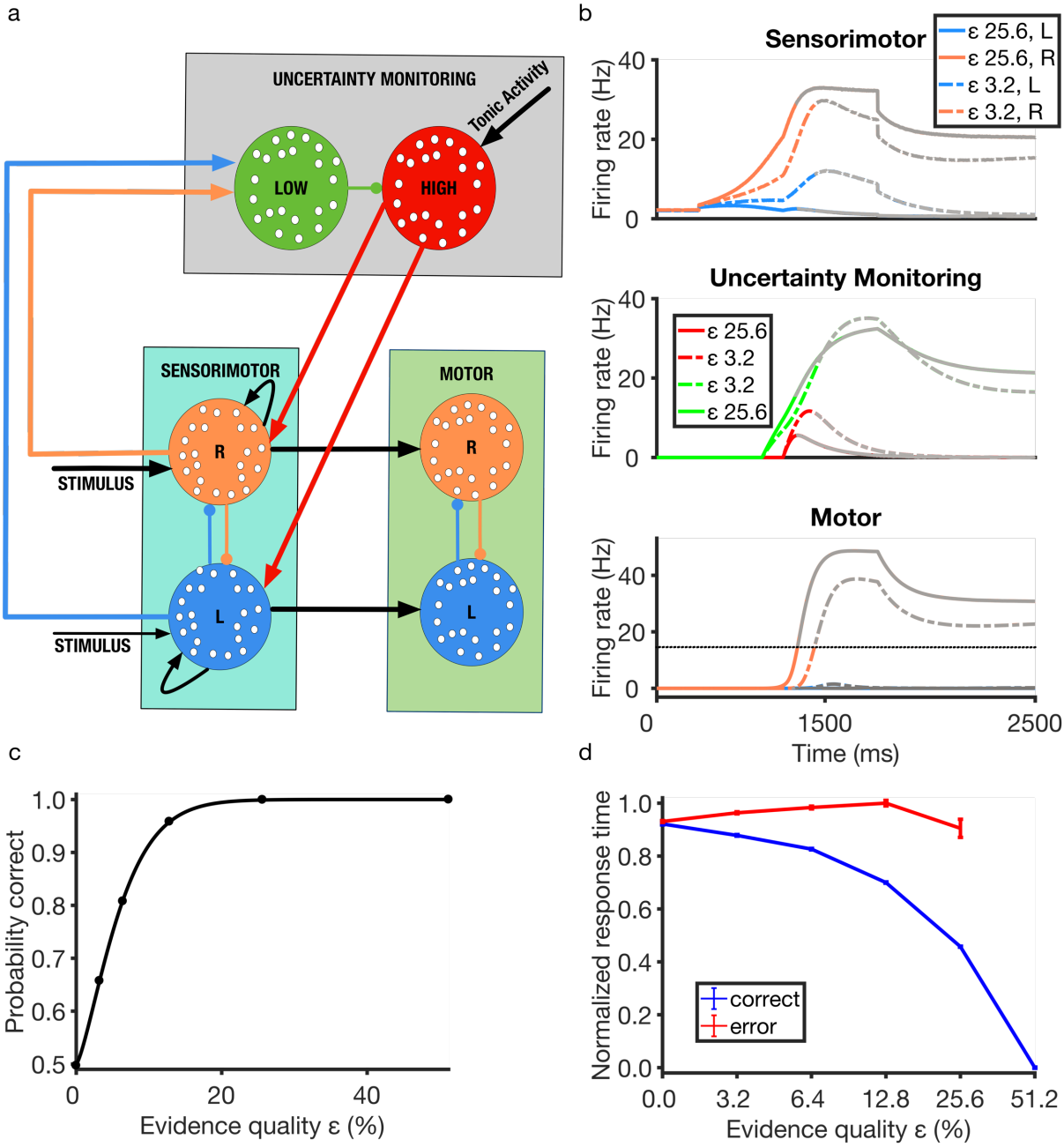

Figure 1 | Schematic diagram and performance of the distributed neural circuit model. (**a**) The model consists of three layers or modules. The uncertainty monitoring module consists of two neuronal populations (a simple cortical column). Low uncertainty encoding neuronal population (green) receives excitatory input (straight arrows) from output of sensorimotor module. It inhibits the high uncertainty encoding neuronal population (lines with filled circles), which in turn provides excitatory feedback to sensorimotor module. The high uncertainty encoding population receives tonic excitatory input which may vary across trials. The sensorimotor module consists of two competing (mutually inhibitory) neuronal populations each selective to noisy sensory information (e.g. rightward or leftward random-dot motion stimulus) favouring one of two (e.g. right R or left L) choice options. The motor module, receiving inputs from sensorimotor module, also consist of neural integrators that report the choice made (**b**) Timecourse of neuronal population firing rates averaged over non-change-of-mind trials with evidence quality, $\varepsilon = 25.6\%$ (easy task; solid lines) and $\varepsilon = 3.2\%$ (difficult task; dashed lines), where ε is equivalent to motion coherence in the classic random-dot stimulus. Faster ramping activity (top and bottom panels) with lower uncertainty quantification (middle panel; red) with larger ε. Colour of activity traces reflect the associated neural populations in (a). To reveal the full network dynamics, the network activities (greyed out) were not reset after a choice was made. (**c**)

Psychometric function used to fit choice accuracy (using a Weibull function, see Methods). (**d**) Response times for correct (blue) and error (red) responses from the model.

The general model behaviour, ultimately reported at the motor neuronal populations, is qualitatively similar to the neuronal firing rates and psychophysical (choice accuracy and response time) data observed in various two-choice reaction time experiments[4,36,37]. Specifically, the neural activity of the winning (sensorimotor/motor) neuronal population ramps up faster for higher evidence quality ($\varepsilon = 25.6\%$ cf. 3.2%; equivalent to motion coherence in random dot stimulus – see Methods) (Fig. 1b, top and bottom panels); accuracy increases monotonically with evidence quality (Fig. 1c) while reaction time decreases (with error choices slower than correct choices) (Fig. 1d; compared with[36,38]). A choice is considered to be made when one of the motor neuronal population activities crosses a prescribed threshold of 17 Hz[34]. The motor neuronal population activity is also directly mapped onto the motor output or positional space (see Methods and below).

Importantly, the high uncertainty-encoding neuronal population's (phasic) activity is higher for trials with higher uncertainty (due to lower evidence quality) (Fig. 1b, middle panel). This rise-and-decay activity around the motor movement onset is consistent with observations from neural recordings in animal and human studies[6,11,25,39]. We shall henceforth use this phasic neural activity as an indicator of decision uncertainty monitoring in real-time, and the temporal integral of its neural activity (i.e. area under the curve as proxy for any downstream neural integrator readout) as a measure of post-decision uncertainty (Methods). Further, a tonic excitatory input to the high-uncertainty encoding population (Fig. 1a) is included to store the within-trial uncertainty to influence decision performance in the subsequent trial[13] (see below and Methods).

Model accounts for relationships among decision uncertainty and psychophysics

We next simulate our network model to replicate the key experimental findings related to decision uncertainty and confidence as discussed in Introduction. As most of the decision

uncertainty and change-of-mind tasks are based on two-choice reaction-time task paradigms, we shall only focus on such paradigms. Our model first replicates choice accuracy decreasing monotonically with uncertainty (Fig. 2a), while producing the 'X pattern'[6] of decision uncertainty (Fig 2b). Decision uncertainty is higher during more difficult tasks, especially ones that more likely lead to error choices.

To explain the results in Figs. 2a and b, we map out a "decision uncertainty space" with respect to the evidence quality and total input to the high uncertainty encoding neuronal population. Based on the (averaged) peak neural activity measure (similar results for the area-under-the-curve measure) of uncertainty, we found that decision uncertainty is more likely to increase when the total input to the high uncertainty-encoding neuronal population and the evidence quality are both low (Figs. 2c and d). More specifically, in correct responses, there are substantial changes on decision uncertainty with respect to evidence quality when compared to the tonic input activity. But both parameters are more equally effective in affecting decision uncertainty for error choices. In the case of correct responses, due to faster response time for higher evidence quality (Fig. 1d, blue), responses are made before temporal integration of sensory evidence in the low uncertainty encoding neuronal population takes place (Supplementary Fig.1, middle panel). This leads to weak inhibition to the high uncertainty-encoding neuronal population, and subsequently leading to lower uncertainty levels. However, for error responses, higher overall levels of excitatory sensory based input are integrated over a longer time by the low uncertainty population due to the relatively slower responses (Fig. 1d, red). This increases the inhibition to the high uncertainty neuronal population, leading to higher uncertainty (Supplementary Fig. 1, middle panel). Furthermore, lower (higher) excitatory feedback to the sensorimotor neurons also causes slower (faster) decisions – a positive feedback effect.

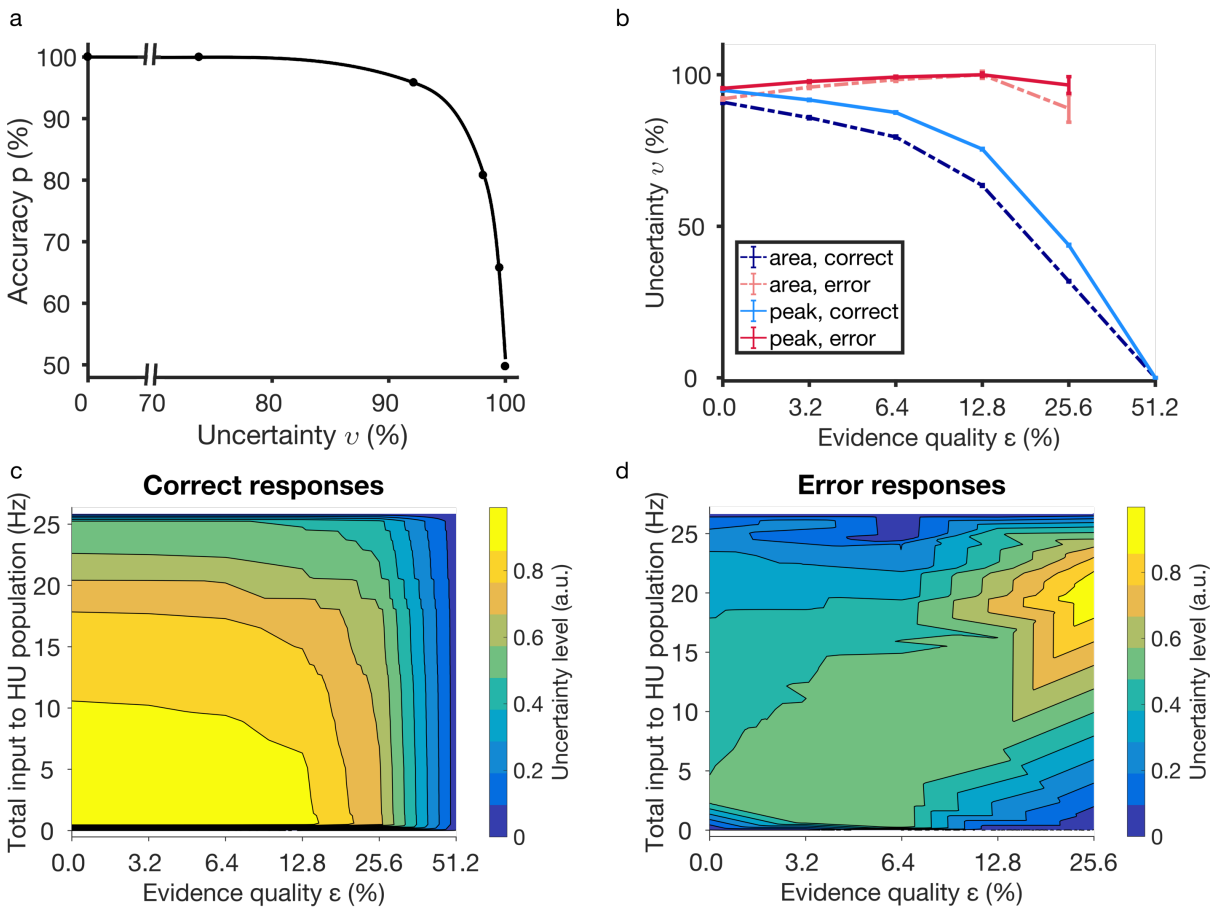

Figure 2 | Model accounts for relationships among decision uncertainty, accuracy and evidence quality. (**a**) Choice accuracy as a function of uncertainty (based on peak of high uncertainty-encoding neuronal population activity). (**b**) Uncertainty as a function of evidence quality. Red (blue): error (correct) choices. Bold (dashed): Uncertainty measure based on averaged peak (peak) or temporal integral (area) of the high uncertainty-encoding neuronal population activity (Methods). Error bars are SEM. (**c**) Uncertainty level with respect to total input to high uncertainty encoding population and evidence quality in case of correct responses. Uncertainty is highest during difficult tasks due to low total input to high uncertainty population caused by strong inhibition from the low uncertainty population. (**d**) Uncertainty level with respect to total input to high uncertainty encoding population and evidence quality for error responses. Uncertainty is highest during easy tasks due to low total input to high uncertainty population caused by strong inhibition from the low uncertainty population. (**c-d**) Uncertainty measured using peak activity (see Methods); similar patterns using its temporal integrated values (not shown).

Previous work using a multi-stage decision task paradigm has shown that the level of uncertainty in making a decision can affect the response times in a subsequent decision – suggested to be a form of optimal strategy[40]. Specifically, this occurs only if the consecutive decisions are correct. By incorporating a simple memory (with decay) mechanism across trials on the tonic excitatory input to the high uncertainty-encoding population (see Methods), our model can replicate this behaviour (Fig. 3a), indicating more time taken in the second decision if the first decision is correct as compared to an error (Fig. 3a). This trend holds

regardless of the evidence quality (task difficulty), with the exception of the easiest difficulty level (due to very low uncertainty levels during these tasks; see Figs. 1d and 2c). The model naturally accounts for this as the neural activity encoding the uncertainty level in the current trial is carried over to the subsequent trial (Methods). This in turn accelerates or decelerates the ramping up of neural activity in the sensorimotor populations and hence decreases or increases the response time, respectively.

If the trials are sorted based on the outcome of both the 1st and 2nd decisions (Fig. 3b), i.e. correct-error combinations, the model predicts substantial differences in response times for error then correct responses in the second decision. Again, this can be explained by Figs. 2c and d. In Fig. 2c for correct responses, the tonic activity effect is moderate as compared to the evidence quality. But for error responses (Fig. 2d), the error responses are more affected by the tonic activity.

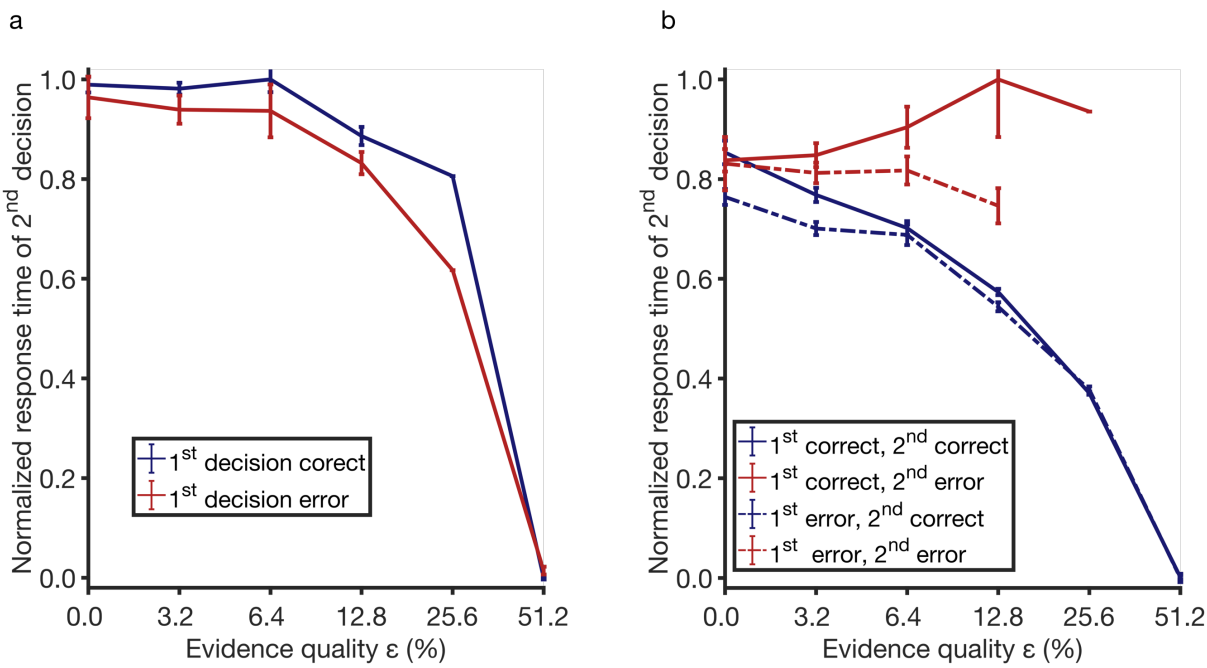

Figure 3 | Model accounts for and predicts how response times are affected by uncertainty in the previous decision. (**a**) Normalized response times of the 2nd decision when the first decision is correct (blue) and error (red). The model exhibits faster response times, when the 1st decision is incorrect as compared to correct, replicating experimental observation. (**b**) Response times of the second decisions are split into error (red) and correct (blue) decisions. Blue bold and dashed lines: Model predicts the difference in response times to be higher when the second choice is an error (red), as compared to correct (correct). Error bars are SEM.

Model accounts for change-of-mind behaviours

Previous studies have shown that change-of-mind during decision-making usually leads to the correction of an impending error[4,33]. Although previous studies have linked change-of-mind to the temporal integration of noisy stimulus[4,33], we demonstrate in our model that change-of-mind is internally generated, and linked to decision uncertainty. Specifically, our model replicates the observation[4,33] that the probability of change-of-mind decreases monotonically with evidence quality with the majority of trials leading to ultimately correct choices (Fig. 4a). Further, and consistent with previous observations[4,33], changes to correct choices peak at intermediate evidence quality level before gradually decreasing (Fig. 4a). Using a fixed maximum duration (of 4 s), our model simulation also shows late (Fig. 4b, solid lines) and early (Fig. 4b, dashed lines) changes-of-mind, depending on whether the target threshold was reached before the change-of-mind occurs (Methods). Moreover, our model predicts that response times are slower when the decisions are change-of-mind, regardless of evidence quality (Fig. 4c). Further prolonging of response times is also found in error choices.

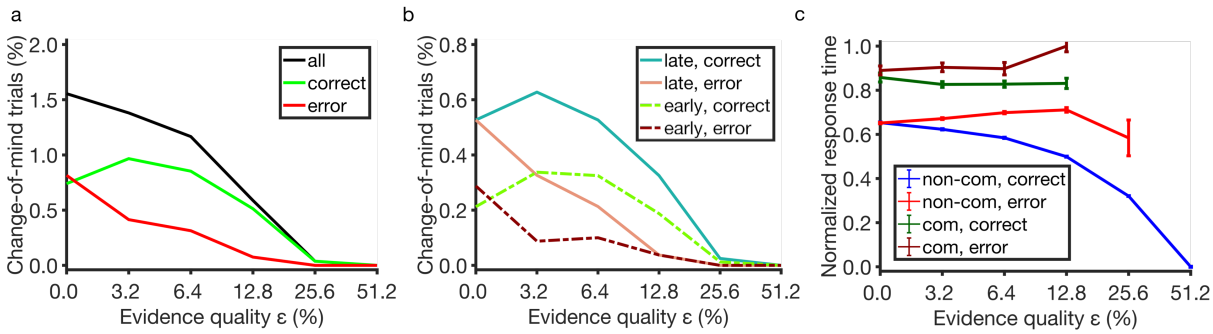

Figure 4 | Model accounts for and predicts key characteristics of change-of-mind. (**a**) Probability of change-of-mind with respect to evidence quality. Black: Total probability of change-of-mind, consisting of both correct and error choices. Green (red): only subsequent correct (error) change-of-mind choices. Probability of change-of-mind for subsequent correct choices peak at $\varepsilon = 3.2$, before decreasing. (**b**) Comparison between early and late change-of-mind trials. Likelihood for change-of-mind for both late and early correct choices peak at the same evidence quality level $\varepsilon = 3.2$. Solid (dashed): Late (early) change-of-mind trials. Late change-of-mind trials are more frequent than early change-of-mind trials (**c**) Response times are slower with decisions consisting of change-of-mind (com) or error choices. Error bars are SEM.

Experimental observation has shown that change-of-mind is associated with reversal of dominance of neural activities over time within a trial[41]. In our model simulation with change-of-mind, there is only a small proportion (~1.2% among all trials) in which the firing-rate activities of the competing sensorimotor neuronal populations distinctly reverse their order of dominance over time within a trial. Fig. 5a (top) shows the trial-averaged activity traces of such reversal condition, which can be directly mapped, via the motor neuronal population activity (Methods), into motor output position, for instance, X position (of saccadic eye or hand movement) (Fig. 5a, bottom). We can observe initial switching of neural activity dominance of the sensorimotor neuronal populations before subsequently being dominated by population 1 (Fig. 5a, top). Note that although the switching of dominance can be small, the difference in activities are integrated and magnified by the motor neuronal populations, leading to an initial bias towards choice 1 (positive X position). Further, it should be noted that both sensorimotor neural activities can return to their spontaneous activities – but the motor neuronal population activity (not shown) could still continue to integrate over time, magnifying the differences in evidences, and hence the motor output position can move towards a choice target (Supplementary Fig. 2)

Neural circuit mechanism of change-of-mind behaviours

Next, we will apply dynamical systems analysis[34] to demonstrate that this reversal phenomenon is caused not only by noise and strong sensory evidence favouring one population over the other, as indicated in previous modelling work[33], but also due to the effective excitatory feedback of the uncertainty-monitoring module. Similar to our previous work[34,42], we plotted the phase planes of the sensorimotor neuronal population activities – which are governed by their slow (NMDA-mediated) population-averaged synaptic gating variables, S_1 and S_2 (Figs. 5b-d). (These gating variables are monotonic functions of their associated neuronal population firing rates[34,42].) The stimulus is presented with low evidence quality with $\varepsilon = 3.2\%$. Shown in blue and orange curves in Figs. 5b-d are the nullclines of the

sensorimotor module, and their intersections are the steady states – the middle saddle-like steady state (or saddle fixed point) in Figs. 5b and d is unstable while the more off-diagonal ones are stable steady states associated with the choices (or choice attractor states) (Methods). For the latter, the choice attractor closer to the S_1 (S_2) axis represents the stable (final) state for making choice 1 (2).

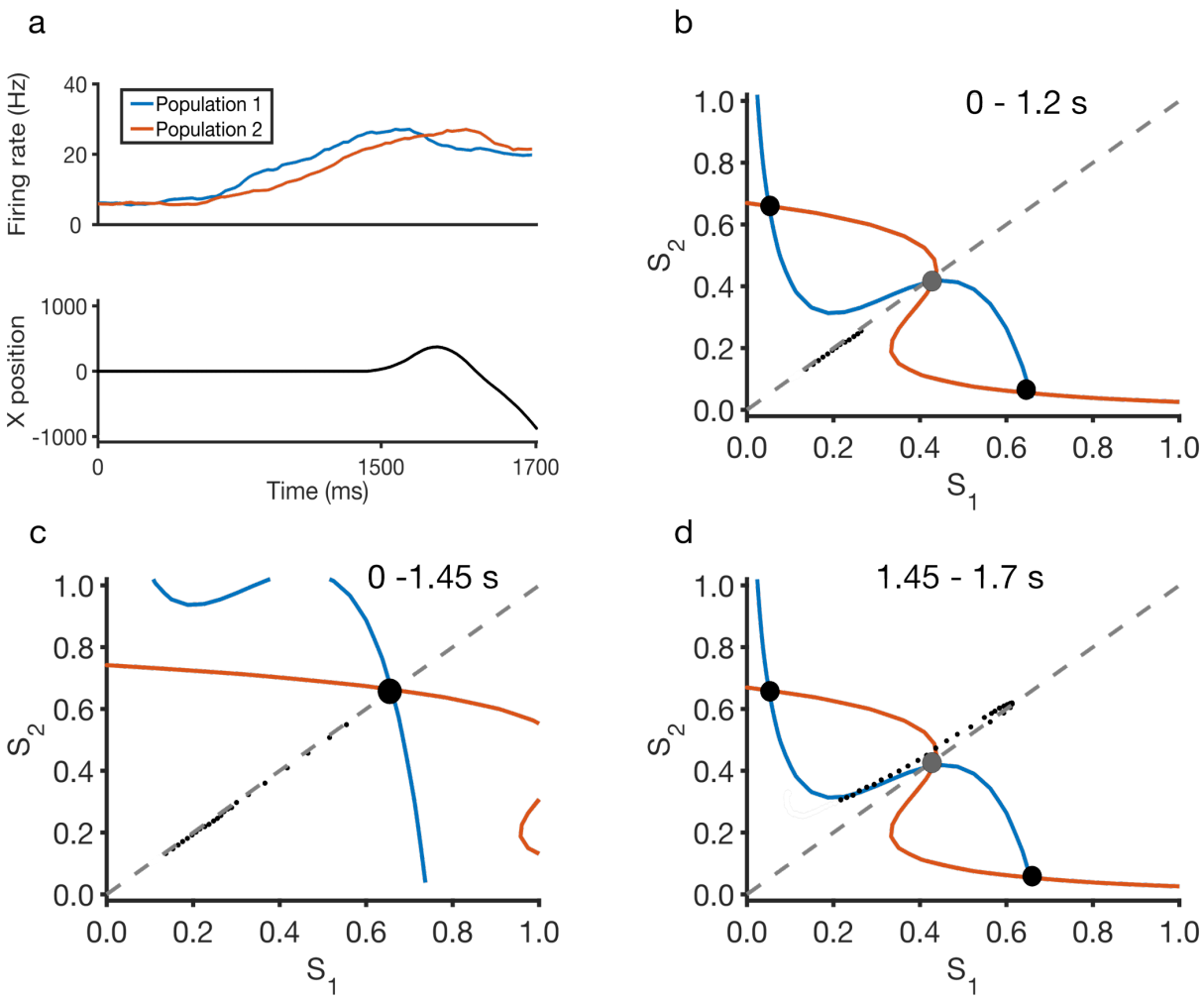

Figure 5. Neural circuit mechanism of early change-of-mind behaviour. (**a**) Mean timecourse of firing rates in sensorimotor module (top panel) and motor trajectory (bottom panel). Left (blue line) and right (orange line) populations compete after stimulus onset. As motor starts moving in one direction (without reaching the target), a reversal of neural activity dominance in sensorimotor module occurs. This leads to early change-of-mind, reflected in the motor module (not shown) and motor position (bottom). (**b**) The initial phase-space of the sensorimotor module immediately upon stimulus onset with small biased input (low evidence quality) with $\varepsilon = 3.2\%$. Blue (S_1) and orange (S_2) lines are the nullclines for the synaptic gating dynamical variables associated with neuronal populations 1 and 2, respectively. Grey filled circle: unstable saddle steady state (fixed point); black filled circle: stable steady state (fixed point) or choice attractor. Grey dashed line: phase-plane diagonal. Time ranges at the top correspond to a specific time epoch during the simulation (**c**) Due to large excitatory uncertainty feedback from the uncertainty monitoring module, the phase plane reconfigures, and a new stable fixed point appears which aid the initially losing population (1). The trajectory (black dots) is now drawn towards this attractor, crossing back the phase plane diagonal. (**d**) Both sensorimotor neuronal populations stop integrating uncertainty input, resulting in the phase plane (nullclines) reverting to the previous condition. Here, a decision is still made by the differential

activity of the motor populations, as they continue to integrate excitatory input from the sensorimotor module (cf. panel 1a).

With a difficult task (small bias in the phase plane), the sensorimotor neuronal populations integrate sensory evidence and ramp up their activities towards one of the two choice attractors, almost along the phase-plane diagonal (Fig. 5c, black dotted trajectory). Fluctuations due to noise contribute mainly to the switching of dominance in the neural activities. Further ramping up of their activities increases the high uncertainty-encoding neuronal population's firing activity and provides excitatory feedback to the sensorimotor module. This leads to the reconfiguration of the phase space and the creation of a new more centralized and choice-neutral stable steady state, to which the state trajectory of the sensorimotor module activity is now drawn (Fig. 5c). Notice that the choice attractors have vanished. The model suggests that this new stable steady state plays an important role in change-of-mind – it allows the losing neuronal population a higher chance of winning the race over the other neuronal population. While these are occurring, the motor module begins temporally integrating any difference in the sensorimotor neural activities.

Due to the transient nature of the high uncertainty-encoding neuronal population activity (Fig. 1c, middle), the excitatory feedback returns to baseline level, and the phase plane reverts back to its initial configuration (Fig. 6a to 6d) (prior to the activation of the uncertainty monitoring module's activity (Fig. 6b)). This causes the trajectory to move towards the higher part of the phase plane and, coupled with noise, leads to a change-of-mind behaviour – reflected in the reversal of motor movement (positive-to-negative) direction (Fig. 5a, bottom). It should be noted that in the model, the final decision is determined by whether the firing rate of motor neural populations, which themselves are neural integrators, reach a prescribed target threshold (see Methods). Thus, change-of-mind could still occur even if activity reversal is not clearly observed in the sensorimotor module.

The above are simulated trials with early changes-of-mind. Late occurrence of change-of-mind can also be explained in our model (~1.2% among all trials). Fig. 6 illustrates the trial-averaged neural dynamics for late change-of-mind trials using the same stimulus. Here, the

reversal in neural activity in the sensorimotor module is clearer than in the previous example (Fig. 6a, top) – activity of neuronal population 1 initially wins before being taken over by that of neuronal population 2. This causes a change-of-mind in the motor module after reaching the choice target in position space (Fig. 6a, bottom). The explanation for the initial epoch of the trial is similar to that for early change-of-mind (Fig. 6b). However, in this case, the activity trajectory early on deviates farther away from the phase-plane diagonal (Fig. 6c), causing the motor output to more quickly reach one of the choice targets (Fig. 6a, bottom). The newly created choice-neutral stable steady state allows the initially losing sensorimotor neuronal population to gain ground (Fig. 6c), and with some fluctuations due to noise, to subsequently win after the new central steady state disappears and the network returns to its previous winner-take-all state (Fig. 6d). This process of choice reversal takes much longer than in the previous type of (early) change-of-mind.

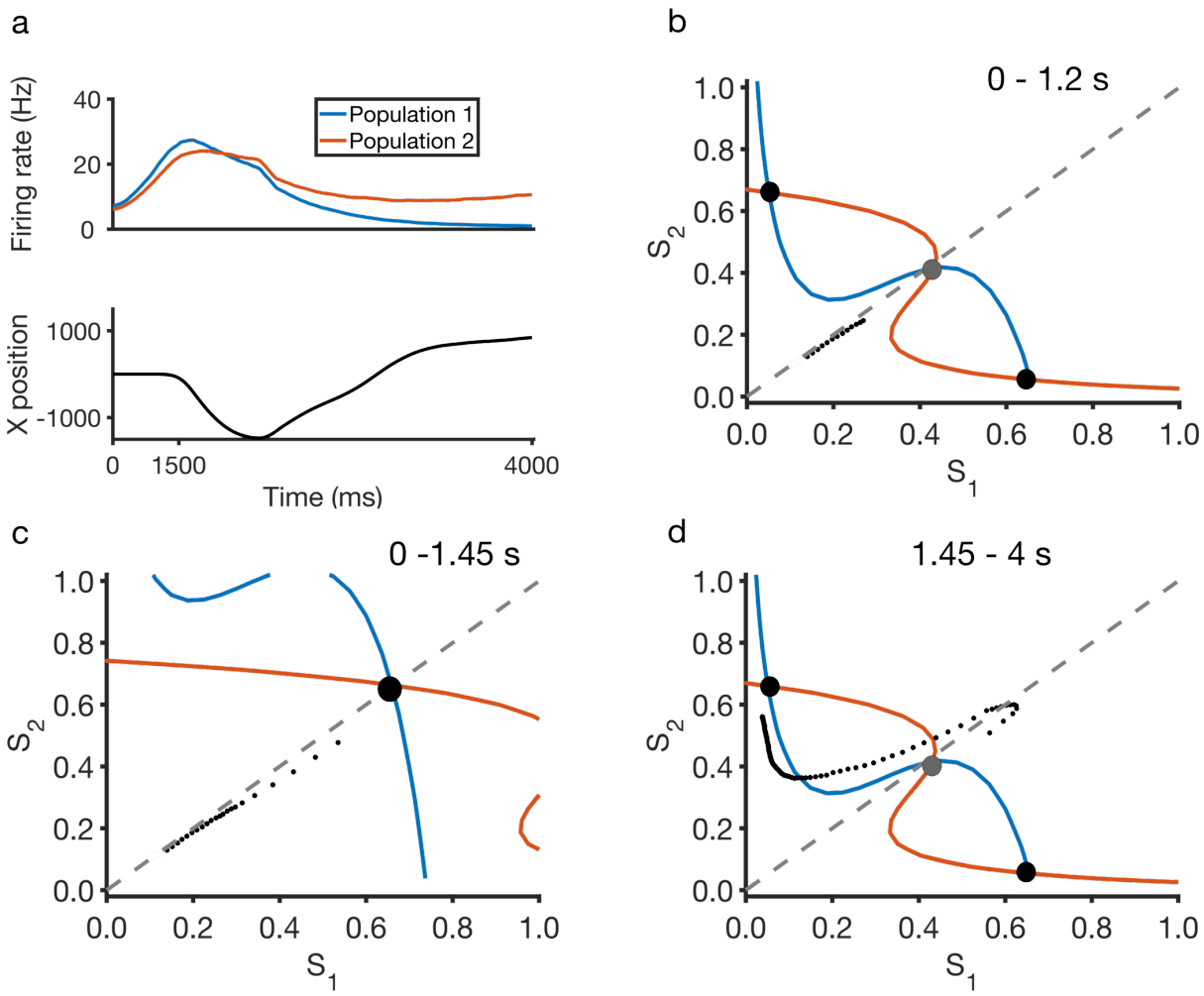

Figure 6. Neural circuit mechanism of late change-of-mind behaviour. (**a**) Mean timecourse of firing rates in sensorimotor module (top panel) and motor trajectory (bottom panel). Left (blue line) and right (orange line) populations compete after stimulus onset. After the motor module reaches the choice target (position 1000), a clear reversal of neural activity in sensorimotor module occurs. This leads to late change-of-mind. (**b**) The phase-space of the sensorimotor module with stimulus and biased input (evidence quality) $\varepsilon = 3.2\%$. (**c**) The trajectory (black dots) is initially drawn towards the centre attractor. (**d**) Phase plane (nullclines) reverting to the previous condition. The complete reversal in activity leads to clear 'neural' change-of-mind at the sensorimotor level.

In our analyses we found that the new central stable steady state is less likely to emerge with higher evidence quality levels due to low excitatory feedback from the uncertainty module (Figs. 2c and d; Supplementary Fig. 1). This explains why higher evidence quality generally leads to lower probability of change-of-mind[4,33] (Figs. 4a and b). For lower evidence quality, the phase plane is almost symmetrical (Fig 5b). Thus, the network is likely to make an error choice initially due to noisy fluctuations. This can lead to longer integration of the decision uncertainty module and providing stronger excitatory feedback – in the form of a transient, centralized attractor state – and consequently, correcting the decision. However, increasing the evidence quality leads to lower probability of change-of-mind (as discussed). This explains the observed peak in probability of correct changes-of-mind (Fig. 4a).

Discussion

We have proposed the first neural circuit computational model that encodes decision uncertainty, the reciprocal form of decision confidence. The model's decision uncertainty can be represented in real-time for online excitatory feedback or post-decision form. The neural model is developed based on transient neural dynamics as observed in animal studies and human neuroimaging studies[6,25], and the relationship between choice certainty and evidence and elapsed time [12,13]. Building on our previous decision-making model[34], our extended neural circuit model can account for several observations commonly found in experimental studies of decision confidence and change-of-mind[4,6,10,33].

First, our model was able to exhibit higher degree of decision uncertainty with more difficult tasks (lower evidence qualities) and lower choice accuracy[6,10,32]. When the simulated

data was sorted into correct and error choices, the model showed higher decision uncertainty with lower evidence quality for correct choices, but counter intuitively with better evidence quality for incorrect choices, in line with the well-known observed X-pattern[6,10,32]. This was explained by the fact that correct choices were faster than error choices, with lesser integration time for the uncertainty-encoding module, which led to lower decision uncertainty. For error choices, the integration time was longer with higher evidence quality. This led to longer integration for the uncertainty-encoding module and higher decision uncertainty. Furthermore, the uncertainty module provided a closed-loop recurrent network mechanism of excitatory feedback with the sensorimotor neuronal population, enhancing the latter's responses. This was reminiscent of dynamic gain or urgency mechanism[43,44]. Future work could test this mechanism. For example, one could use a task paradigm that produces fast error choices[45] and determine whether the X-pattern is absent.

By storing the decision uncertainty from the previous trial in the tonic excitatory input to the high uncertainty-encoding neuronal population (Fig. 1a), the model could naturally account for behavioural performances in multi-stage decision task paradigm of decision confidence[40]. Specifically, the model showed that decision uncertainty from a correct previous trial caused a slower response time as compared to that when a previous trial was incorrect (Fig. 3a). Moreover, when the second decision was split into correct and error choices, the model predicted that a previous decision affected the response times of subsequent error choices more than subsequent correct choices (Fig. 3b), which could be easily checked or tested in experiments.

These could be explained by the uncertainty space in Figs. 2c and d, which showed that for correct responses, tonic excitatory input to the high uncertainty population (Fig. 3c) had smaller influence on decision uncertainty as compared to evidence quality. However, for error responses, both factors had similarly strong influence on decision uncertainty. In the model, since the uncertainty was carried over, influencing the tonic excitatory input, the across-trial effect was weaker for the subsequent correct than for error choices. Future work could test this prediction, together with its neural correlates. Direct microstimulation or

inactivation of the associated neurons may further provide causal information.

The same model could exhibit changes-of-mind which were more likely to occur when the decision tasks were more difficult[4,33]. Specifically, the model showed that changes-of-mind were more often accompanied by correcting an initial impending error choice – hence more error-to-correct changes than correct-to-error changes, consistent with previous observations[4,33], and that the likelihood of changes-of-mind to the correct choice slightly peaked at intermediate level of task difficulty before rapidly decreasing as the task becomes easier[4,33] (Figs. 4a and b). The model was also able to produce early and late changes-of-mind behaviours (Figs. 4b and c).

We used phase-plane analysis to explain these phenomena. First, the process of change-of-mind can be understood in terms of the sensorimotor network state being attracted to three distinct basins of attraction: basin of attraction of the initial choice, then to the basin of the central choice-neutral 'uncertain' state, and finally to the basin of attraction of the other choice. With higher evidence quality, we found that the correct choice attractor dominated the phase plane (with its larger basin of attraction, Supplementary Fig. 6), and the central attractor was less likely to appear due to the low uncertainty-based excitatory feedback. This explains the monotonic decrease of the probability of change-of-mind (Fig. 4a). In other words, changes-of-mind did not occur due to the heavily biased phase plane. However, at low evidence quality levels ($\varepsilon < 4\%$), the phase plane was almost symmetric (Fig. 5b), which led to more initial errors. Under such low evidence quality, it was increasingly likely that the network would make an initial error choice[34]. This led to longer integration of the decision uncertainty module and providing stronger excitatory feedback – in the form of a transient, centralized choice-neutral stable stead state – and eventually, correcting the decision. On the contrary, increasing the evidence quality leads to lower probability of changes. This explains the peak in probability of correct changes-of-mind (Fig. 4b). The model further suggested that during early changes-of-mind, noisy fluctuations around the phase-plane diagonal led to subtle deviations early in the trial (Fig 5). The downstream motor module, which is itself a neural integrator, magnified these deviations and led to movement being

initiated toward a choice target. However, late changes-of-mind were caused by earlier excursions from the phase-plane diagonal which could lead to positioning the motor output on the initial choice target[4].

Fig. 7 illustrates a hypothetical decision 'potential well'[34] that summarizes our key findings for change-of-mind behaviour – the centralized attractor, caused by the excitatory feedback from the decision uncertainty module, and coupled with noise, can allow an initial impending choice to be altered. The strength and duration of this attractor depends on the evidence (and elapsed time) for temporal integration by the sensorimotor neuronal populations. Unlike previous neurocomputational models[33,46], our model does not rely explicitly on reversing the stimulus input to neural populations or having a relatively low (first) decision threshold (to induce faster errors). Further, it does not rely on abstract mathematical calculation of decision uncertainty[28]. Inspired by neural evidence of decision confidence[6,11,21], we have a dedicated neural module that automatically monitors and quantifies the decision uncertainty. This module has a plausible circuit architecture that resembles, to some extent, a simple cortical column. With this structure, our model predicts that there is an "anti" uncertainty neuron – the low uncertainty-encoding neurons. Future neurophysiological and neuroanatomical studies could identify the presence and functions of such neurons (e.g. in the frontal cortex).

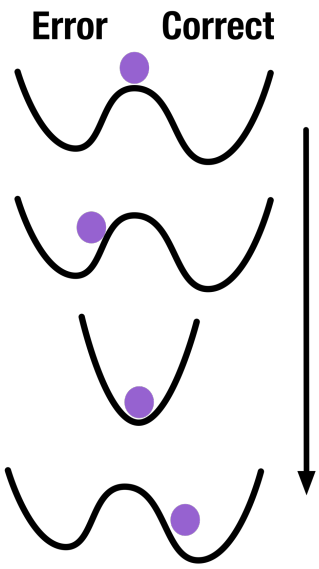

Figure 7. Conceptual illustration of change-of-mind due to decision uncertainty. Top-to-bottom: Hypothetical "potential well" of the network changes over epochs within a trial (arrow). When making a choice between two alternatives, the strength of the stimulus (and noise) drives the ball towards one of the two wells (in this case, an error choice). A transient strong excitatory input (due to the excitatory feedback from the uncertainty module) changes the "energy" landscape into one centralized deep well, allowing a higher chance to change its initial decision.

Unlike other computational models of perceptual decision confidence or change-of-mind[4,10,27], our extended neural circuit is more realistic by involving more brain regions. Evidence shows perceptual decisions are performed and distributed across multiple brain regions[47]. In particular, our model has a motor module in which its activity can be directly transformed to motor positional coordinates. This allows us to explicitly identify early and late change-of-mind responses generated by the model, and their underlying neural mechanisms. With this multi-modular model, we found that neural correlates of change-of-mind (switching of neural activity dominance[41]) can occur in the motor layer without a clear or complete reversal in more upstream sensory or sensorimotor neurons. Thus, our model suggests that change-of-mind behaviour may be more clearly identified in more motor-based than sensory areas[37].

In summary, our work has provided the first neural circuit model that can compute decision confidence or uncertainty within and across trials, while also occasionally exhibiting changes-of-mind. The model not only can replicate several important observations of decision confidence and change-of-mind but also is sufficiently simple to allow rigorous understanding of its mechanisms. Taken together, our modelling work has shed light on the neural circuit mechanisms underlying decision confidence and change-of-mind.

Methods

Psychometric and chronometric function. We used a Weibull function[48] to fit the psychometric function, $p = 1 - 0.5\ exp(-\varepsilon/\alpha)^{\beta}$, where p is the probability of a correct choice, ε is the evidence quality, which, in the case of the random-dot stimulus[49,50], is equal to the motion coherence level (c'). With the parameters used with our model (see Table 1), α

(the threshold at which the performance is 85%) is set to 6.59%, while β, the slope, is equal to 1.35. We defined the model's response (or reaction) time as the overall time it took for the motor neuronal population activity to reach a threshold value of 17 Hz (mimicking a motor output and physically reaching a choice target) from stimulus onset time. This is equivalent to the motor position reaching some threshold value (see below).

Modelling sensorimotor populations using two-variable model. We used the reduced version of the spiking neural network model[46] described by its two slowest dynamical variables, which are the population-averaged NMDA-mediated synaptic gating variables[34]. The dynamics of the two neuronal populations can be described by:

$$\frac{dS_1}{dt} = -\frac{S_1}{\tau_s} + (1 - S_1)\gamma H(x_1, x_2) \quad (1)$$

$$\frac{dS_2}{dt} = -\frac{S_2}{\tau_s} + (1 - S_2)\gamma H(x_2, x_1) \quad (2)$$

where the two excitatory neuronal populations representing the two choice options are labelled 1 and 2, and the S's are the population-averaged NMDA-mediated synaptic gating variables. γ is some fitting constant. τ_S denotes the synaptic gating time constant (100 ms) constrained by NMDA receptor physiology. H denotes the nonlinear single-cell input-output function fitted to that of a spiking neuronal model. The firing rates of the sensorimotor populations can be described by these three equations:

$$H_i = \frac{ax_i - b}{1 - e^{-d(ax_i - b)}} \quad (3)$$

$$x_i = J_{N,ii}S_i - J_{N,ij}S_j + I_0 + I_i + J_{mc0}y_{HU} \quad (4)$$

$$I_i = J_{A,ext}\,\mu_0\left(1 \pm \frac{\varepsilon}{100\%}\right) \quad (5)$$

where a, b, d are parameters for the input-output function fitted to a leaky integrate-and-fire neuronal model [34]. The dynamical variables S_i and S_j are from Eqs. 1 and 2. $J_{N,ii}$ and $J_{N,ij}$ are synaptic coupling constants from recurrent connections. I_0 denotes a constant value that

represents an effective bias input from the rest of the brain. I_i denotes the excitatory stimulus input to population i, and is proportional to the evidence quality ε, with the stimulus strength constant denoted by μ_0: $I_i = J_{A,ext}\,\mu_0\left(1 \pm \frac{\varepsilon}{100}\right)$. $J_{A,ext}$ represents the external synaptic coupling constant. In addition to the features in the previous work[34], the strength of excitatory feedback from the high uncertainty population is controlled by J_{mc0}. Hence, decision uncertainty is monitored and fed back to the sensorimotor populations via excitatory feedback.

Uncertainty monitoring neuronal populations. Two neural populations mimicking canonical cortical microcircuit were implemented. One is selective to low decision uncertainty while another to high uncertainty. Their dynamics are described by:

$$\tau_{mc}\frac{dy_{LU}}{dt} = [J_{VLU}(H_i + H_j) - g]_+ - y_{LU} \quad (6)$$

$$\tau_{mc}\frac{dy_{HU}}{dt} = [\mu - J_{N,HULU}\,y_{LU} - g]_+ - y_{HU} \quad (7)$$

where $[\,]_+$ denotes a threshold-linear input-output function, with its input argument in units of nA. J_{VLU} denotes a synaptic coupling constant from the sensorimotor populations to the low-uncertainty encoding neuronal population. H_i and H_j are the neuronal population firing rates from the sensorimotor populations i, j. g represents some top-down inhibition (1000 nA) on the uncertainty-monitoring populations from beginning of trial, which is removed 300 ms and 400 ms from Eqs. (6) and (7) after stimulus onset, respectively. When the activity of one of the sensorimotor neuronal populations crosses a threshold value $(35\ Hz)$, g is reactivated (3000 nA). This results in the activity pattern of uncertainty-monitoring module to mimic data observed in neural recordings[6,25] (see Fig. 1b, middle panel). $J_{N,HULU}$ denotes the inhibition strength from the low-uncertainty to high-uncertainty neuronal populations, while μ is some excitatory constant biased input that can be modulated by decision confidence from previous trial (see below).

Motor neuronal populations. Similar to the uncertainty-monitoring neuronal populations, we dynamically modelled the motor output module using threshold-linear functions. Two neural populations selective for right and left - with mutual inhibition - were used. The persistent activity is maintained using mutual inhibition to create a line attractor model[51]. The dynamics of the neuronal populations for the two choices (1 and 2) are described by:

$$\tau_h \frac{dy_L}{dt} = [J\, H_1 - J_{N,LR}\, y_R - g]_+ - \, y_L \qquad (8)$$

$$\tau_h \frac{dy_R}{dt} = [J\, H_2 - J_{N,RL}\, y_L - g]_+ - \, y_R \qquad (9)$$

where H_1 and H_2 are the firing rates from the two corresponding sensorimotor populations (Fig. 1), and the associated coupling constant $\mathrm{J} = 1$ *nA Hz*$^{-1}$. $J_{N,ij}$ denotes a coupling constant from population i to population j. The negative sign indicates connectivity is effectively inhibitory. As for the uncertainty module, g represents some top-down inhibition (1000 nA) on the motor populations from beginning of trial, and is removed when the activity of one of the sensorimotor neuronal populations crosses a threshold value $(35\ Hz)$. The motor module output as a position in the x directional space is approximated by a linear function:

$$x = n(\mathrm{y_L} - \mathrm{y_R}) \qquad (10)$$

where n is a constant scaling factor with value of 55.

Uncertainty within a single trial. We used two measures to quantify the level of decision uncertainty in a trial. For the first measure, we used the maximum firing rate value of the high uncertainty-encoding population for each trial n, allowing real-time monitoring of decision uncertainty. For a specific evidence quality value, we calculated the trial-averaged and SEM of these maximal values. For the second measure, we calculated the area under the curve of the firing rate activity over time of the high uncertainty-encoding population using the trapezoidal numerical integration scheme for each trial n. This provides an overall quantification of decision confidence after a choice is made. It also acts as a proxy for any

downstream neural integrator that temporally integrates real-time decision uncertainty information. Again, for each evidence quality value, we calculated the mean and SEM of the areas. Either measure of decision uncertainty is then normalised using feature scaling to bring all values within the range [0,1]. This is done by:

$$X' = \frac{X - X_{min}}{X_{max} - X_{min}} \quad (11)$$

Uncertainty across coupled trials. In coupled trials, the evidence quality of the second trial was selected probabilistically from a uniform distribution, where $\varepsilon \in [0, 3.2, 6.4, 12.8, 25.6, 51.2]$. The area under the curve of the summed activity of the high uncertainty population at trial n , X_n , is transformed and stored into some activity measure C in the subsequent trial. We used a simple linear transformation described by

$$C_{n+1} = \alpha X_n + \beta \quad (12)$$

where n denotes the trial number, α and β are scaling parameters. The parameter values set in this work are $\alpha = 0.00035\, nA$ and $\beta = 0.5\, nA$. This value of C_{n+1} is then used to modulate the tonic input (and hence baseline activity) of the high uncertainty-encoding population (μ, in equation (7)) in the second trial using the following update:

$$\mu \rightarrow \mu + C_{n+1} \quad (13)$$

Regression and classification of model outputs. We used a linear polynomial function to fit the model's decision accuracy as function of uncertainty function as follows:

$$p = \tau \,.\, \upsilon + \theta \quad (14)$$

where p is the probability of a correct choice, υ is the normalised uncertainty value (equation 14). The model behaviour is identified to have a change-of-mind if there is a reversal in order of dominance between the two motor neuronal population firing rates, i.e. if there is a change in sign of $\mathrm{y_L} - \mathrm{y_R}$ (see Figs 6a and 5a) with an absolute magnitude of 1 Hz. If this reversal occurs after reaching a choice target (of 17 Hz), it is classified as a late change-of-

mind; otherwise it will be classified as early change-of-mind. The reversal in activity leads to change-of-mind if and only if the opposite target threshold is reached.

Simulation and analysis. The code to simulate the model was written in MATLAB (version 2016b) and was run on a Mac OS X workstation. The forward Euler-Maruyama numerical integration scheme an integration time step of 0.1 ms was used for numerical integration of the dynamical equations (describing dynamics within a trial). Smaller time steps were checked (e.g. 0.01 ms) without affecting the results. XPPAUT[52] was used to perform dynamical systems (phase-plane) analysis and for parameter search on each neural module. The model's parameter values are summarized in Supplementary Table 1. The model was simulated under a response-time task paradigm with a timeout of 4s. The stimulus appeared 800ms after a trial began. Only 1.8% of total simulated trials (8000 trials per condition) were indecision trials in which the motor activity did not cross the 17 Hz threshold, i.e. choice target was not reached. These simulated trials were discarded and not included in our analyses.

Code availability. MATLAB and XPPAUT code used to simulate the model and generate the figures can be found at this private GitHub repo: https://github.com/nidstigator/uncertainty_com_submission. README includes instructions on how to reproduce these figures. Please request to be a collaborator of this private repo in order to view and download the source code files.

Data availability. Data used as part of this work was generated by simulating a custom computer code. This code is made available upon request from the editor and/or reviewers. Our code availability statement outlines how to gain access to this code.

References

1. Pouget, A., Beck, J. M., Ma, W. J. & Latham, P. E. Probabilistic brains: knowns and unknowns. *Nat. Neurosci.* **16,** 1170–1178 (2013).
2. Tversky, A. & Kahneman, D. Judgment under uncertainty: Heuristics and biases. *Science (80-.).* **185,** 1124–1131 (1974).
3. Glimcher, P. W. *Decisions, uncertainty, and the brain: The science of neuroeconomics*. (MIT press, 2004).
4. Resulaj, A., Kiani, R., Wolpert, D. M. & Shadlen, M. N. Changes of mind in decision-making. *Nature* **461,** 263–266 (2009).
5. Rabbitt, P. M. Errors and error correction in choice-response tasks. *J. Exp. Psychol.* **71,** 264 (1966).
6. Kepecs, A., Uchida, N., Zariwala, H. a & Mainen, Z. F. Neural correlates, computation and behavioural impact of decision confidence. *Nature* **455,** 227–231 (2008).
7. Kiani, R. & Shadlen, M. N. Representation of confidence associated with a decision by neurons in the parietal cortex. *Science* **324,** 759–764 (2009).
8. Meyniel, F., Sigman, M. & Mainen, Z. F. Confidence as Bayesian Probability: From Neural Origins to Behavior. *Neuron* **88,** 78–92 (2015).
9. Pouget, A., Drugowitsch, J. & Kepecs, A. Confidence and certainty: distinct probabilistic quantities for different goals. *Nat. Neurosci.* **19,** 366–374 (2016).
10. Beck, J., Ma, W., Kiani, R. & Hanks, T. Probabilistic population codes for Bayesian decision making. *Neuron* **60,** 1142–1152 (2008).
11. Lak, A. *et al.* Orbitofrontal cortex is required for optimal waiting based on decision confidence. *Neuron* **84,** 190–201 (2014).
12. Kiani, R., Corthell, L. & Shadlen, M. N. Choice certainty is informed by both evidence and decision time. **100,** 130–134 (2014).
13. Fetsch, C. R., Kiani, R., Newsome, W. T. & Shadlen, M. N. Effects of cortical microstimulation on confidence in a perceptual decision. *Neuron* **83,** 797–804 (2014).
14. Fetsch, C. R. *et al.* The influence of evidence volatility on choice , reaction time and confidence in a perceptual. *Elife* 1–31 (2016). doi:10.7554/eLife.17688
15. Rahnev, D. A., Maniscalco, B., Luber, B., Lau, H. & Lisanby, S. H. Direct injection of noise to the visual cortex decreases accuracy but increases decision confidence. *J. Neurophysiol.* **107,** 1556–1563 (2012).
16. Grimaldi, P., Lau, H. & Basso, M. A. There are things that we know that we know, and there are things that we do not know we do not know: Confidence in decision-making. *Neurosci. Biobehav. Rev.* **55,** 88–97 (2015).
17. O'Connell, R. G., Shadlen, M. N., Wong-Lin, K. & Kelly, S. P. Bridging Neural and Computational Viewpoints on Perceptual Decision-Making. *Trends Neurosci.* (2018). doi:10.1016/j.tins.2018.06.005
18. Yeung, N. & Summerfield, C. Metacognition in human decision-making: confidence and error monitoring. *Philos. Trans. R. Soc. Lond. B. Biol. Sci.* **367,** 1310–21 (2012).
19. Fleming, S. M., Ryu, J., Golfinos, J. G. & Blackmon, K. E. Domain-specific impairment in metacognitive accuracy following anterior prefrontal lesions. *Brain* **137,** 2811–2822 (2014).
20. Hanks, T. D. & Summerfield, C. Perceptual decision making in rodents, monkeys, and humans. *Neuron* **93,** 15–31 (2017).
21. Gherman, S. & Philiastides, M. G. Neural representations of confidence emerge from the process of decision formation during perceptual choices. *Neuroimage* **106,** 134–143 (2015).

22. Fiser, J., Berkes, P., Orbán, G. & Lengyel, M. Statistically optimal perception and learning: from behavior to neural representations. *Trends Cogn. Sci.* **14,** 119–130 (2010).
23. Griffiths, T. L., Chater, N., Kemp, C., Perfors, A. & Tenenbaum, J. B. Probabilistic models of cognition: exploring representations and inductive biases. *Trends Cogn. Sci.* **14,** 357–364 (2010).
24. McClelland, J. L. *et al.* Letting structure emerge: Connectionist and dynamical systems approaches to cognition. *Trends Cogn. Sci.* **14,** 348–356 (2010).
25. Murphy, P. R., Robertson, I. H., Harty, S. & O'Connell, R. G. Neural evidence accumulation persists after choice to inform metacognitive judgments. *Elife* **4,** 1–23 (2015).
26. Rounis, E., Maniscalco, B., Rothwell, J. C., Passingham, R. E. & Lau, H. Theta-burst transcranial magnetic stimulation to the prefrontal cortex impairs metacognitive visual awareness. *Cogn. Neurosci.* **1,** 165–175 (2010).
27. Pleskac, T. J., Busemeyer, J. R. & others. Two-stage dynamic signal detection: a theory of choice, decision time, and confidence. *Psychol. Rev.* **117,** 864 (2010).
28. Link, S. CS Pierce, confidence and random walk theory. in *Proceeding of the Nineteenth Annual Meeting of the International Society ofr Psychophysics. Stockholm, Sweden: International Society for Psychophysics* (2003).
29. Ratcliff, R. A theory of memory retrieval. *Psychol. Rev.* **85,** 59–108 (1978).
30. Ratcliff, R. & Rouder, J. N. Modeling response times for two-choice decisions. *Psychol. Sci.* **9,** 347–356 (1998).
31. Fleming, S. M. Changing our minds about changes of mind. *Elife* **5,** e14790 (2016).
32. Wei, Z. & Wang, X.-J. Confidence estimation as a stochastic process in a neurodynamical system of decision making. *J. Neurophysiol.* **114,** 99–113 (2015).
33. Albantakis, L. & Deco, G. Changes of mind in an attractor network of decision-making. *PLoS Comput. Biol.* **7,** (2011).
34. Wong, K.-F. & Wang, X.-J. A Recurrent Network Mechanism of Time Integration in Perceptual Decisions. *J. Neurosci.* **26,** 1314–1328 (2006).
35. Wilson, H. R. & Cowan, J. D. Excitatory and inhibitory interactions in localized populations of model neurons. *Biophys. J.* **12,** 1–24 (1972).
36. Roitman, J. D. & Shadlen, M. N. Response of neurons in the lateral intraparietal area during a combined visual discrimination reaction time task. **22,** 9475–9489 (2002).
37. Kaufman, M. T., Churchland, M. M., Ryu, S. I. & Shenoy, K. V. Vacillation, indecision and hesitation in moment-by-moment decoding of monkey motor cortex. *Elife* **4,** e04677 (2015).
38. Shadlen, M. & Newsome, W. Neural basis of a perceptual decision in the parietal cortex (area LIP) of the rhesus monkey. *J. Neurophysiol.* **86,** 1916–1936 (2001).
39. Fleming, S. M., van der Putten, E. J. & Daw, N. D. Neural mediators of changes of mind about perceptual decisions. *Nat. Neurosci.* (2018). doi:10.1038/s41593-018-0104-6
40. van den Berg, R., Zylberberg, A., Kiani, R., Shadlen, M. N. & Wolpert, D. M. Confidence is the bridge between multi-stage decisions. *Curr. Biol.* **26,** 3157–3168 (2016).
41. Kiani, R., Cueva, C. J., Reppas, J. B. & Newsome, W. T. Dynamics of neural

population responses in prefrontal cortex indicate changes of mind on single trials. *Curr. Biol.* **24,** 1542–1547 (2014).
42. Wong, K.-F., Huk, A. C., Shadlen, M. N. & Wang, X.-J. Neural circuit dynamics underlying accumulation of time-varying evidence during perceptual decision making. *Front. Comput. Neurosci.* **1,** 6 (2007).
43. Ditterich, J. Evidence for time-variant decision making. *Eur. J. Neurosci.* **24,** 3628–3641 (2006).
44. Niyogi, R. K. & Wong-Lin, K. Dynamic excitatory and inhibitory gain modulation can produce flexible, robust and optimal decision-making. *PLoS Comput. Biol.* **9,** (2013).
45. Ratcliff, R., Smith, P. L. & McKoon, G. Modeling regularities in response time and accuracy data with the diffusion model. *Curr. Dir. Psychol. Sci.* **24,** 458–470 (2015).
46. Wang, X. J. Probabilistic decision making by slow reverberation in cortical circuits. *Neuron* **36,** 955–968 (2002).
47. Schall, J. D. Macrocircuits: Decision networks. *Curr. Opin. Neurobiol.* **23,** 269–274 (2013).
48. Quick, R. F. A vector-magnitude model of contrast detection. *Biol. Cybern.* **16,** 65–67 (1974).
49. Ball, K. & Sekuler, R. A specific and enduring improvement in visual motion discrimination. *Science (80-.).* **218,** 697–698 (1982).
50. Newsome, W. T., Britten, K. H. & Movshon, J. A. Neuronal correlates of a perceptual decision. *Nature* (1989).
51. Gonçalves, P. J., Arrenberg, A. B., Hablitzel, B., Baier, H. & Machens, C. K. Optogenetic perturbations reveal the dynamics of an oculomotor integrator. *Front. Neural Circuits* **8,** 1–22 (2014).
52. Ermentrout, B. Phase plane: the dynamical systems tool. *Pacific Grove, CA Brooks/Cole.* (1990).